Supporting Information

$MgIn_2S_4$ decorated MOF-derived C/N-CeO_2 nanorod heterojunction as efficient photocatalyst towards H_2O_2 production reaction and H_2 evolution reaction

Jayashree Panda[a], Pragyandeepti Behera[a], Satyabrata Subudhi[a], Suraj Prakash Tripathy[a], Gayatri Swain[a], Srabani Dash[a], Kulamani Parida[a]*

Centre for Nano Science and Nanotechnology, Siksha "O" Anusnadhan (Deemed to be University), Bhubaneswar-751030, Odisha, India

E-mail: Corresponding author: kulamaniparida@soa.ac.in

Supporting Information Contents:

No. of Pages: 17

No. of Figures: 12

No. of Tables: 8

No of equation: 2

1. Materials and methods:

1.1 Chemicals utilized: Cerium chloride [$CeCl_3.7H_2O$], 2-Amino-1, 4-benzeen dicarboxylic acid [$H_2BDC\text{-}NH_2$], Magnesium nitrate [$Mg\ (NO_3)_2.\ 6H_2O$], Indium nitrate [$In\ (NO_3)_2.xH_2O$], Thioacetamide [CH_3CSNH_2] were purchased from sigma Aldrich. Methanol, and N, N- Dimethyl formamide (DMF) were obtained from MERCK and are used without further purification.

1.2 Synthesis Route of C/N-CeO_2, MIS, and C/N-CeO_2/MIS:

1.2.1 Synthesis Route of Ce-MOF and derived C/N-CeO_2:

Ce based SBUs coordinated with amine ($-NH_2$) group functionalized BDC linkers to prepare the MOF which is synthesised by hydrothermal technique. In this preparation strategy, 0.74 g of $CeCl_3.7H_2O$ and 0.36 g of $H_2BDC\text{-}NH_2$ were dissolved in 30 mL of DMF separately, followed by each solution being stirred (30 min) to obtain Ce-metal and $BDC\text{-}NH_2$ ligand precursor solution for MOF preparation. The obtained Ce salt solution was mixed with the prepared $H_2BDC\text{-}NH_2$ solution and subjected to stirring for 60 min. Then, the pale-yellow suspension was transferred into a Teflon-lined stainless-steel autoclave and kept in the hot air oven for 24 h at 150 °C for hydrothermal treatment. Subsequently the autoclave was allowed to cool down naturally, and the sample was collected by centrifugation. Further, the obtained product was activated in methanol and washed several times with methanol (to remove unreacted metal salts and ligands). Thereafter, the material was dried overnight at 343 K and finally the off white-coloured sample was ground and labelled as Ce-MOF. To synthesize the C/N-CeO_2 photocatalysts, the as-prepared Ce-MOFs were calcined in a muffle furnace for 2 h at a heating rate of 5 °C min^{-1} from room temperature (RT, 25°C) to 450 °C under ambient air atmosphere.

1.2.2. Synthesis Route of MIS:

In a usual procedure, first $Mg\ (NO_3)_2.6H_2O$ and $In\ (NO_3)_3.xH_2O$ were dissolved in a beaker containing 50 mL of distilled water under ultra-sonication for 1 hour at room temperature. Afterwards CH_3CSNH_2 solution in DI was added slowly to the above suspension and kept under ultra-sonication for another 30 minutes. For this purpose the ratio of Mg: In: S should be maintained in accordance to 1:2:8. Then, the clear suspension was transferred into a Teflon-lined stainless-steel autoclave and hydrothermally treated at 180 °C for 12 hours. Subsequently

the autoclave was allowed to cool down naturally, and the sample was then centrifuged and washed with water and ethanol each three times, followed by drying in an oven to form the orange coloured desired product.

1.2.3. Synthesis Route of C/N-CeO_2/MIS (MC-x) Heterostructure:

For the synthesis of composites MC-x, first of all, 0.3 g of the as-synthesised C/N-CeO_2 was dispersed in 40 mL of distilled water through ultrasonication for almost 30 minutes (solution–A). Meanwhile, in another beaker calculated amounts of $Mg(NO_3)_2 \cdot 6H_2O$ and In $(NO_3)_3 \cdot xH_2O$ were mixed in a ratio of 1:2 (Mg/In) with 20 mL of distilled water and stirred for 30 minutes (solution–B). Then, aqueous solution of C_2H_5NS was added slowly to the solution–B by maintaining the proportion as 1:2:8 (Mg/In/S) under ultrasonication for 30 minutes, followed by stirring at room temperature for 30 minutes. Thereupon, both solution-A and B was intermixed with stirring for another 30 minutes. Subsequently, the suspension was placed in a 100 mL Teflon-lined stainless-steel autoclave and hydrothermally treated at 180 °C for 12 hours. The sample was then centrifuged and washed with water and ethanol each three times, followed by drying in an oven to form the 10, 20, and 30 wt % MIS decorated on C/N-CeO_2, C/N-CeO_2/MIS composites denoted as MC-x where, x = 1, 2, 3 respectively. The schematic synthesis protocol of all fabricated photocatalysts was displayed in scheme-1.

2. Characterization Details:

2.1. Physicochemical Characterization:

X-ray diffraction study (XRD) of prepared samples were estimated in 2θ range of 5°-80° by Rigaku Ultima IV instrument equipped with Cu Kα X-ray source (λ = 0.154 nm). JASCO V-750 spectrophotometer was used to study the optical property of synthesized samples, taking $BaSO_4$ as the reference. Morphology and internal topological behavior of C/N-CeO_2, MIS, and C/N-CeO_2/MIS was determined via ZEISS SUPRA-55 (Scanning electron microscopy (SEM) and JEOL JEM 2100 (Transmission electron microscopy (TEM) instruments. VG microtech multilab ESCA 3000 spectrometer fitted with Mg-Kα-X-ray source for XPS characterization and ICP-OES analysis was performed with the help of Elementar Vario EL III Carlo Erba 1108 elemental analyser to investigate the binding energy change and determine the wt % of element present in target photo catalyst respectively. Surface texture i.e. N_2 adsorption desorption, surface area and pore distribution of prepared photocatalyst was analysed by NOVA2200e, Quantachrome Apparatus at de-gassing temperature 200 ºC for 7 hrs. Agilent 7890B GC and

the column is HP-5MS was used for GC-analysis of target product i.e. biphenyl. Multi-channel IVIUMnSTAT was used for electrochemical characterization of the synthesized photo catalyst in presence of 0.1 M Na_2SO_4 aqueous solution.

2.2 Electrochemical characterization:

Working electrodes were prepared using the drop casting process over fluorine doped tin oxide (FTO) glass. The FTOs were first thoroughly cleaned using ultrasonication in deionized water and ethanol before being dried in a hot air oven at 100°C. The sample was then applied to the conducting surface of the FTO (1 mg photocatalyst, 1.4 mL ethanol, 40 μL nafion, and 1.6 mL distilled water, all sonicated for 30 min). A typical three-electrode cell is used for electrochemical measurements, with the platinum electrode serving as a counter, the saturated Ag/AgCl electrode serving as the reference electrode, and the sample coated FTO serving as the working electrodes, respectively. The entire analysis was completed in an aqueous solution of 0.1 M Na_2SO_4.

3. Photocatalytic Experimental Setup:

The above synthesized materials were carried out for three types of photocatalytic applications as explained below:

3.1. Photocatalytic H_2O_2 production setup:

The photocatalytic H_2O_2 production reaction of C/N-CeO_2, MIS, and C/N-CeO_2/MIS-2 photocatalysts was carried out in an oxygen saturated atmosphere under UV-Visible light irradiation for 2 hour. For this H_2O_2 evolution experiment, 20 mg of each photocatalyst were dispersed in 20 mL of solution (18mL DI + 2mL Isopropanol) followed by ultrasonication for 15 minutes. Furthermore, at room temperature only, the solution was illuminated with 250 W Hg-lamp followed by oxygen purging for 45 minutes. The suspension was centrifuged and filtered to obtain clear filtrate for analysis after 2 h of photocatalytic reaction. After that, 2 mL of clear filtrate was mixed with 2 mL of 0.1 M potassium iodide and 0.05 mL of 0.01 M ammonium molybdate solution for colour generation before running the spectra. Keeping at rest in dark for 5-10 minutes, the resultant mixture was analysed using a UV-Vis spectrophotometer centred at 350 nm.

3.2. Photocatalytic H_2 evolution setup:

The photocatalytic proficiency of the fabricated binary composite towards hydrogen (H_2) evolution was detected in a gas-closed quartz batch reactor of 100 mL capacity. Typically, 20 mg of photocatalyst powder were dispersed in 20 mL of 10 % (v/v) methanol-water solution, and a 150 W Xe arc lamp was used as the light source, which was kept at a suitable distance from the reaction mixture. Prior to light illumination, the reactor was degassed by purging N_2 gas for 1 h to remove O_2 from the system. Also, continuous stirring condition was maintained throughout the reaction period using a magnetic stirrer to avoid coagulation of nanoparticles. The amount of H_2 evolved after 1 h of light irradiation was calculated by using the downward displacement of water technique. The blank experiment suggested that there is no evolution of hydrogen in absence of light and photocatalyst displaying the pivotal role of both for the H_2O reduction reaction.

3.3. Photocatalytic O_2 evolution setup:

Further the photocatalytic water oxidation activity was evaluated for the as synthesised material using another reactor fitted with a chiller and a light source (UV-Visible light). For this experiment, 20 mg of catalyst was poured in the quartz container and 20 mL of 0.05M $AgNO_3$ solution was added to it, followed by stirring for 30 minutes in dark condition in order to maintain the adsorption-desorption equilibrium. After that, N_2 gas was bubbled through the solution for 30 minutes for deaeration purpose to ensure the oxygen evolved during the processes is due to water splitting reaction only. Further, a 150 W Xe arc lamp was used as light source to irradiate light in the suspension for 1 h. Then, the produced oxygen was quantified by an Agilent 7890b-series GC instrument equipped with the necessary items. Moreover, the apparent conversion efficiency (ACE) for H_2 and O_2 evolution and solar to chemical conversion efficiency (SCC) for H_2O_2 production using the best photocatalyst was evaluated with detailed calculation as below.

4. Calculation of Apparent Conversion Efficiency (ACE)

(a) ACE of MC-2 composite towards H_2 evolution (419.24 μmol h^{-1}) under light irradiation (150W Xe arc lamp) was calculated by the formula as stated below. [S1]

$$\Rightarrow \textbf{ACE} = \frac{Stored\ chemical\ energy\ (SCE)}{Incident\ light\ Intensity\ (ILI)} \quad \text{---------- (S1)}$$

SCE = No. of moles of H_2 produced per sec. * Heat of combustion in kJ/mole (ΔHc of H_2)

= 0.11646 * 10^-6 mole/sec * 285.8 * 10^3 J/mole

= 33.284 * 10^-3 J/sec

= 0.03328 W

ILI = Intensity of used Hg lamp * Distance of lamp from solution * Surface area of the spherical region (2πr) on which light is focused

= 70mW/ cm^2 * 3.14 * (1.5cm)^2

= 494.55 mW

= 0.4945 W

ACE = $\frac{0.03328\ W}{0.4945\ W}$ = 6.73 %

(b) ACE of MC-2 composite towards O_2 evolution (210.09 μmol h^{-1}) under light irradiation (150W Xe arc lamp) was calculated by the formula as stated above. [1]

SCE = No. of moles of O_2 produced per sec. * Heat of combustion in kJ/mole (ΔHc of O_2)

= 0.05835 * 10^-6 mole/sec * 285.8 * 10^3 J/mole

= 16.676 * 10^-3 J/sec

= 0.01667 W

ILI = Intensity of used Hg lamp * Distance of lamp from solution * Surface area of the spherical region (2πr) on which light is focused

= 70mW/ cm^2 * 3.14 * (1.5cm)^2

= 494.55 mW

= 0.4945 W

ACE = $\frac{0.01667\ W}{0.4945\ W}$ = 3.37 %

(c) **Calculation of solar to chemical conversion efficiency (SCC %)**

SCC of MC-2 towards H_2O_2 generation under 250 W Hg-lamp can be calculated by following the equation below [2]:

⇨ **SCC %** = $\frac{\Delta G^{\circ}\ for\ H_2O_2 generation\left(\frac{J}{mol}\right) \times H_2O_2\ produced\ (mol)}{Input\ energy\ (W)\ \times\ reaction\ time\ (s)} \times 100$ ------ (S2)

Further, for H_2O_2 evolution, ΔG° is 117 kJ·mol^{-1}. The irradiance of 250 W Hg-lamp is 1.33 Wcm^{-2} and irradiated area is 84.78 cm^2. In a 1 h of reaction time, the amount of H_2O_2 produced is 56.25 μmol.

Input Energy (W) = Irradiance (W cm^{-2}) * Irradiated area (cm^2)

= 1.33 * 127.17

= 169.13 W

Putting all these in equation [2], the SCC efficiency is calculated to be 0.11%.

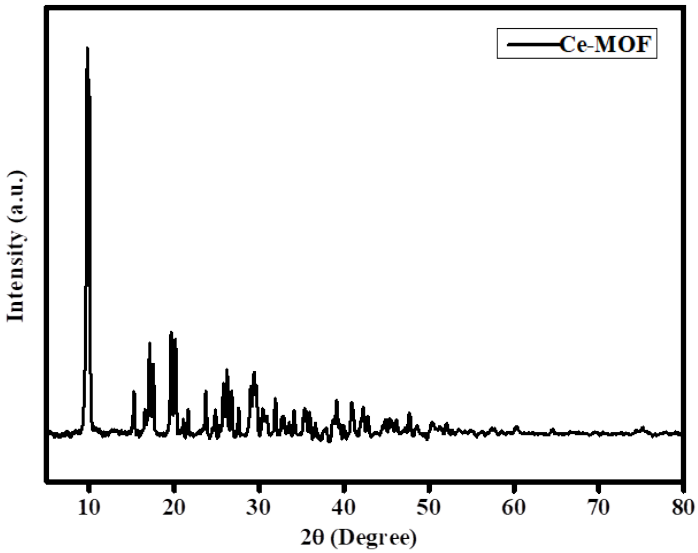

Fig. S1. PXRD pattern of Ce-MOF.

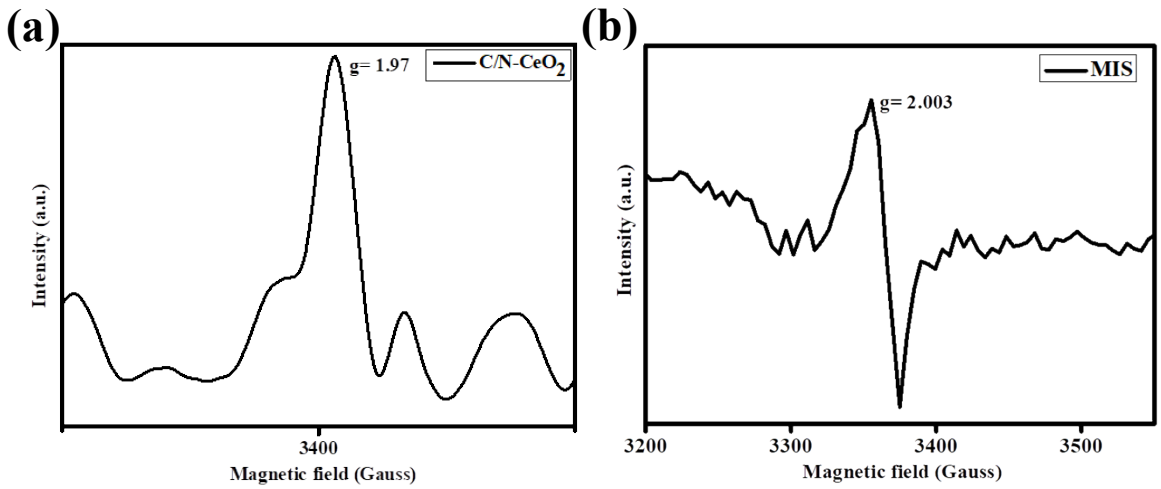

Fig. S2. EPR Spectra of (a) C/N-CeO_2, (b) MIS.

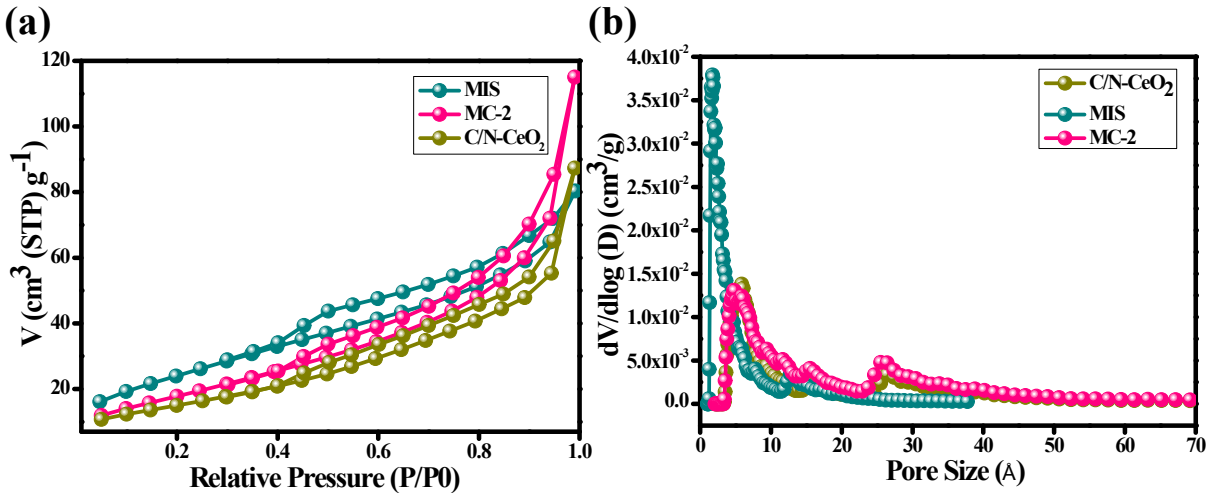

Fig. S3. a) BET surface area and (b) pore size distribution of C/N-CeO_2, MIS, and MC-2.

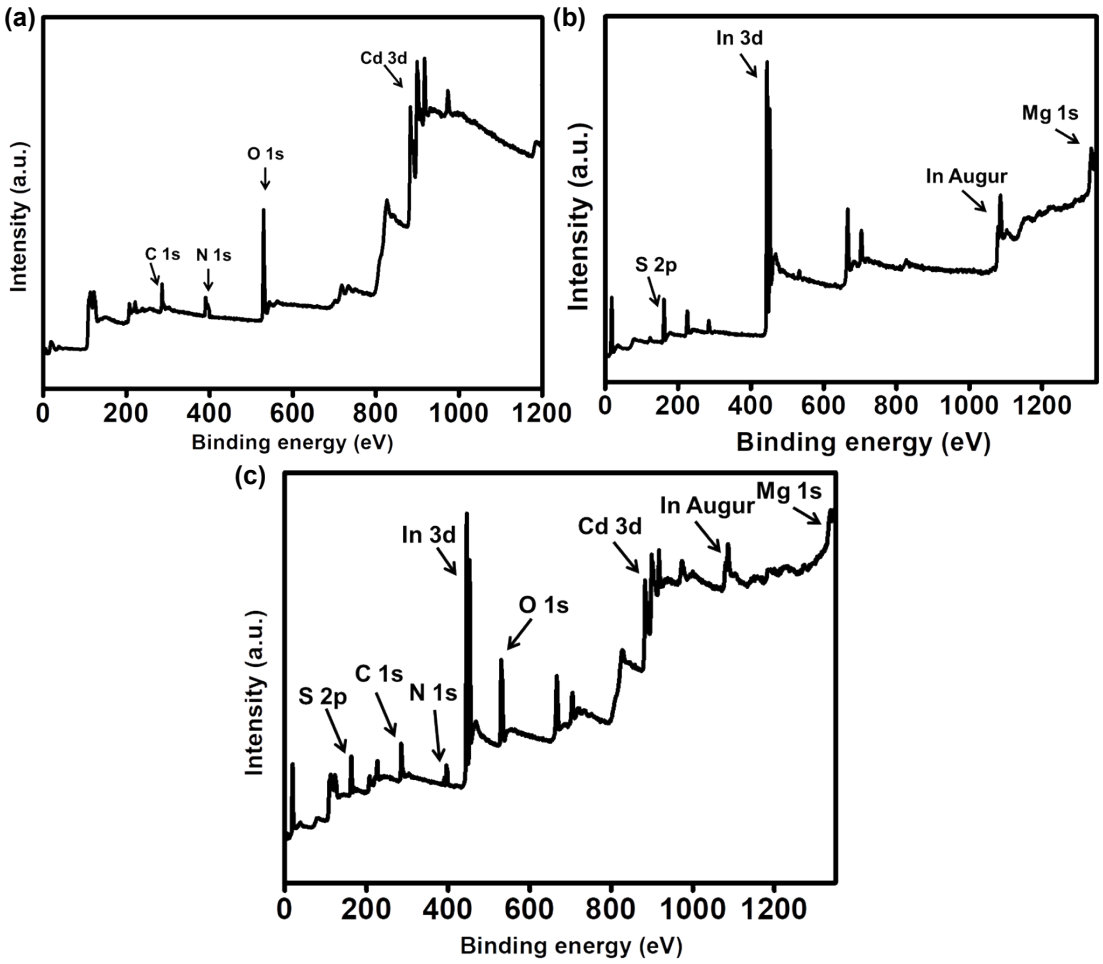

Fig. S4. XPS survey scan spectra of (a) C/N-CeO_2, (b) MIS, and (c) MC-2

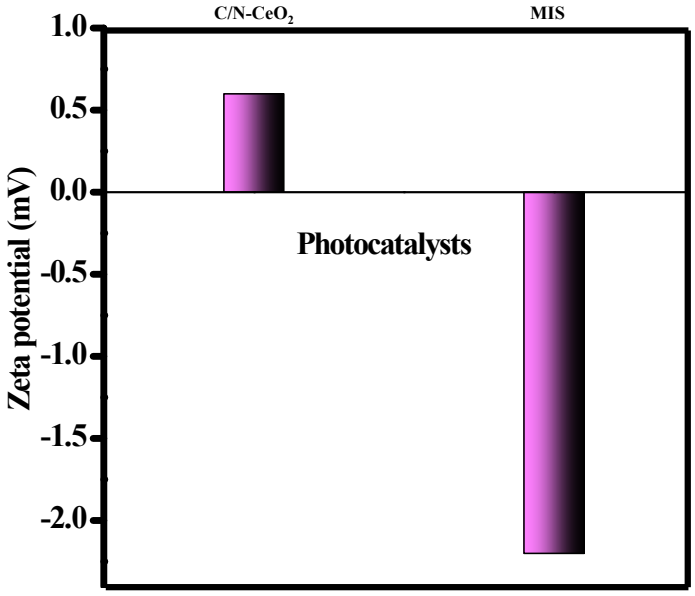

Fig. S5. Zeta potential plot of C/N-CeO_2 and MIS

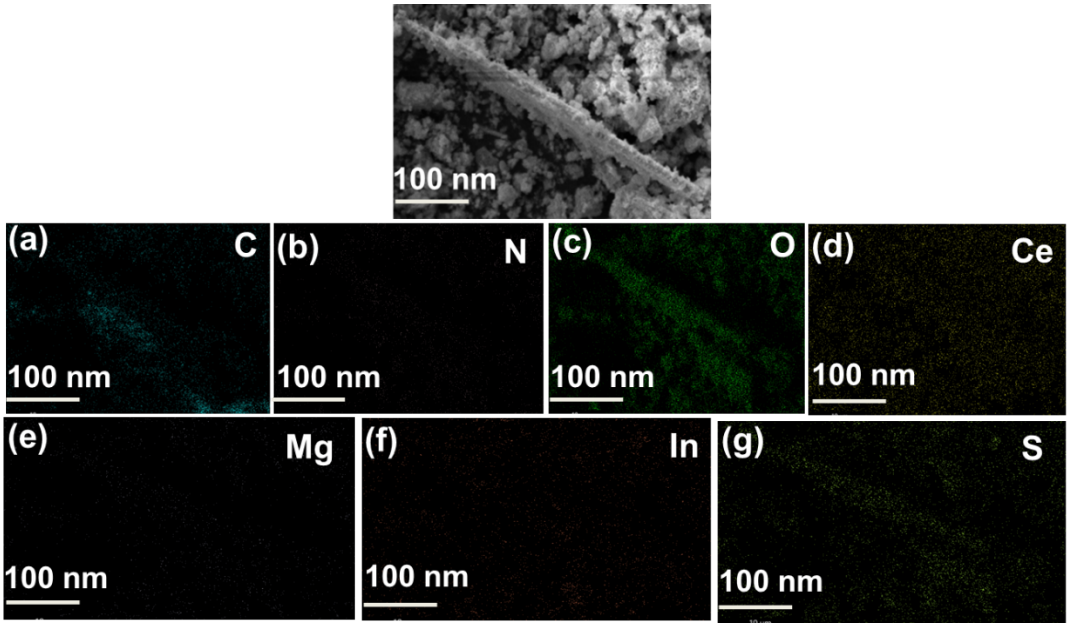

Fig. S6. EDS mapping of the element distribution in MC-2.

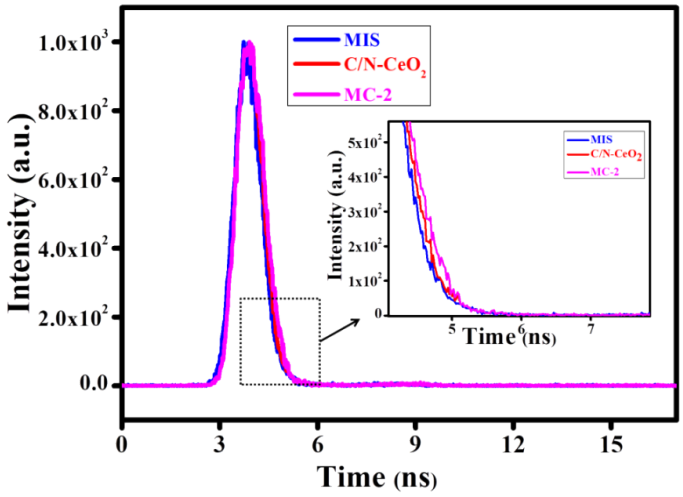

Fig. S7. TRPL plot of C/N-CeO_2 and MC-2 composite

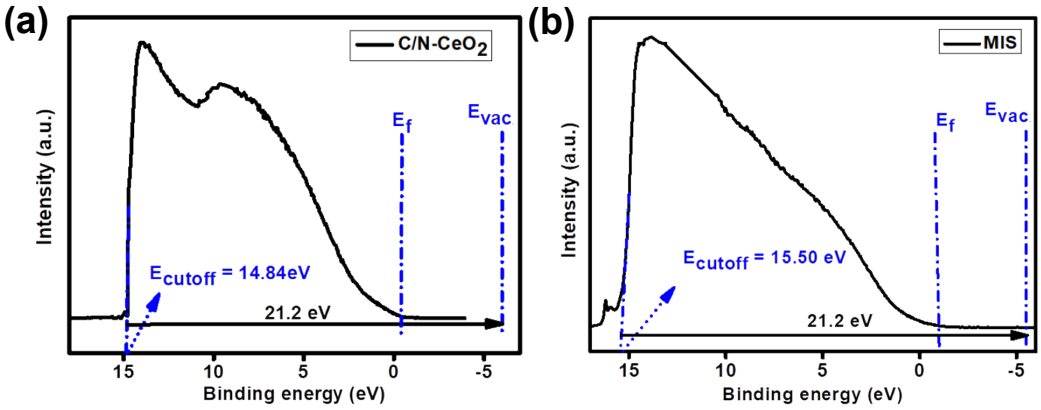

Fig. S8. Ultraviolet photoemission spectroscopy (UPS) spectra of (a) C/N-CeO_2 and (b) MIS

Table S1. XPS binding energy comparison between C/N-CeO_2, MIS, and MC-2 photocatalyst.

Binding energy									**Ref.**
Ce 3d									
C/N-CeO_2	882.4	884.1	889.1	898.4	901.1	900.7	906.5	916.8	[1,2]
MC-2	882.5	884.9	889.5	898.5	901.1	901.3	907.2	916.9	
Difference	0.1	0.8	0.4	0.1	0.0	0.6	0.7	0.1	
Reason	$^3d_{3/2}$	$^3d_{3/2}$	$^3d_{3/2}$	$^3d_{3/2}$	$^3d_{5/2}$	$^3d_{5/2}$	$^3d_{5/2}$	$^3d_{5/2}$	
O 1s									
C/N-CeO_2	529.5		531.3			------			[1,3]
MC-2	529.7		531.9			533.2			
Difference	0.2		0.6			------			
Reason	Lattice oxygen		Oxygen vacancy			Surface adsorbed oxygen			
N 1s									
C/N-CeO_2	399.37				401.12				[4]
MC-2	399.40				401.15				
Difference	0.03				0.03				
Reason	Doped N				Interstitial N				
C 1s									
C/N-CeO_2	284.85		286.1			289.2			[1,5]
MC-2	284.95		286.29			288.9			
Difference	0.1		0.19			0.3			
Reason	C=C		C-N			C-OH, O=C-O			
Mg 1s									
MIS	1305.22								[6,7]
MC-2	1304.86								
Difference	0.36 eV								
Reason	Mg^{+2}								
In 3d									
MIS	444.65				452.23				[6,8]
MC-2	444.42				452.01				
Difference	0.23				0.22				
Reason	$3d_{5/2}$				$3d_{3/2}$				
S 2p									
MIS	161.91				162.98				[6,7]
MC-2	161.85				162.96				
Difference	0.06				0.02				
Reason	$2p_{3/2}$				$2p_{1/2}$				

5. Scavenger test:

The trapping test was conducted to identify the active species which are responsible for the photocatalytic generation of H_2O_2 reaction. Different scavengers such as p-benzoquinone (p-BQ), isopropyl alcohol (IPA), citric acid (CA), and dimethyl sulfoxide (DMSO) are used to verify the presence of reactive species: $^{\bullet}O_2^-$,$^{\bullet}OH$, h^+, and e^- respectively. As we know that CA is used as holes (h^+) scavenger and DMSO as electrons (e^-) scavenger, the role of different reactive species towards photocatalytic H_2O_2 production was examined and displayed in Fig. S6. According to the trapping experiment test, a significant reduction in the production efficiency of H_2O_2 was observed while using DMSO, p-BQ as scavenging agent which demonstrates the principal role of e- and $^{\bullet}O_2^-$ for reduction of O_2 through the 2-electron single step and 1-electron two step processes. Moreover, the production of H_2O_2 moderately affected using IPA and CA as scavenging agent, displaying the minute role of $^{\bullet}OH$ and h^+ as a source of H_2O_2 production.

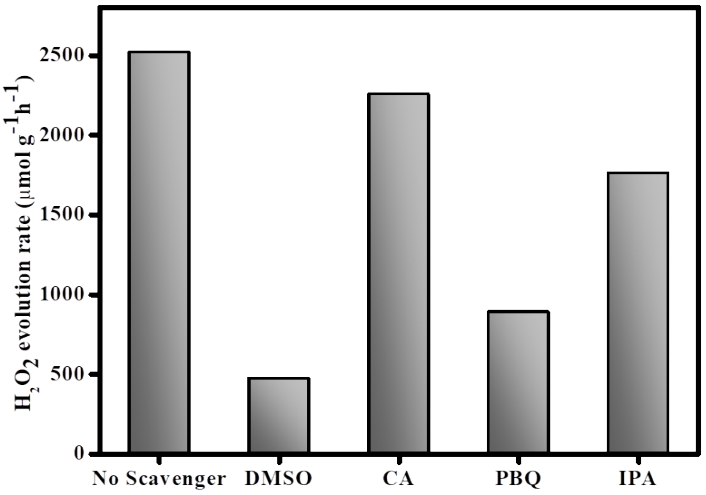

Fig. S9. Photocatalytic H_2O_2 production rate in presence of different scavengers.

Over the catalyst horizon, to confirm the presence of $^{\bullet}O_2^-$ which is the key reactive species towards H_2O_2 production and water reduction, NBT test was conducted. In this typical experiment, 10 mL of Nitro blue tetrazolium suspension ($5*10^5$ M) with 0.01 g photocatalyst was exposed to sunlight for 1 h. After the illumination period, photocatalyst was separated by centrifugation and analyzed through UV-Vis DRS as shown in Fig. S9 (b). From the spectra it can be observed that, solar light exposed NBT shows decreased absorption intensity as compare to the neat NBT which prove the presence of $^{\bullet}O_2^-$ and hence it helps in photocatalytic production of H_2O_2 via O_2 reduction process.

Whereas, to confirm the presence of $^{\bullet}OH$, terephthalic acid (TA) test was performed for the water oxidation reaction. In this experiment, TA reacts with OH^- to form

hydroxyterephthalic acid (HTA), which confirms the presence of •OH in the solution. For this test, 5 mM TA was taken along with NaOH and the required amount of photocatalyst was added to the solution. The final solution was placed under sunlight for 30 min and after that, PL measurement was performed. The emission peak of composite at k = 425 nm is considered as the formation of HTA complex. Above result as shown in Fig. S7 (a) concluded the presence of •OH in the reaction vessel which helped in O_2 evolution reaction via water splitting and moderately helps for H_2O_2 production by combining with another radical of its own.

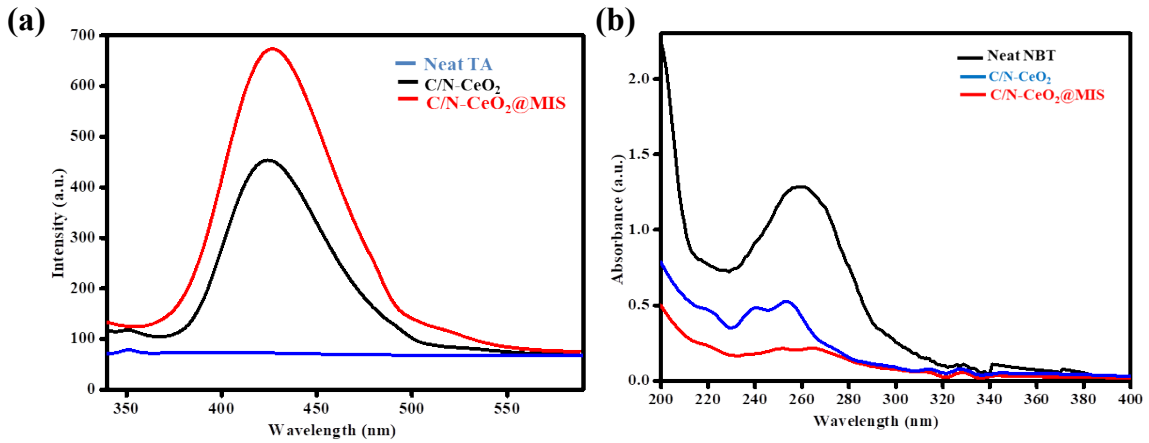

Fig. S10. (a) TA and (b) NBT Test results for neat C/N-CeO_2, and MC-2

Table S2. BET surface area and pore volume of C/N-CeO_2, and MC-2 photocatalysts.

Photocatalyst	**BET surface area (m^2/g)**	**Pore volume (Å)**			
C/N-CeO_2	57.045	2.31	5.54	8.98	14.99
MC-2	71.427	2.04	4.73	7.89	11.49

Table S3. Respective band edge potential and optical bandgap values of C/N-CeO_2 and MIS.

Photocatalyst	**E_{fb} vs Ag/AgCl (V)**	**CB vs NHE (V)**	**VB vs NHE (V)**	**Bandgap (eV)**
C/N-CeO_2	-0.65	2.3	-0.56	2.86
MIS	-1.35	0.91	-1.26	2.17

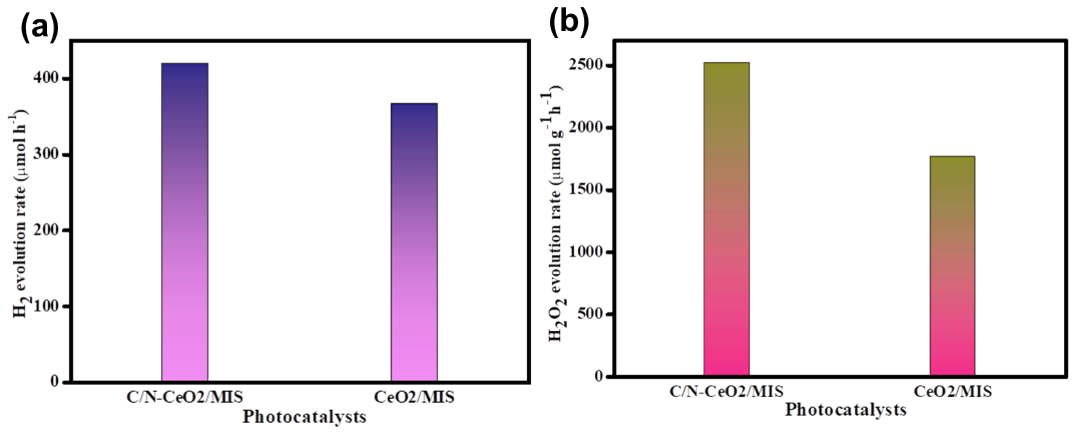

Fig. S11. Comparative photocatalytic H_2 and H_2O_2 production rate using C/N-CeO_2/MIS and CeO_2/MIS composites.

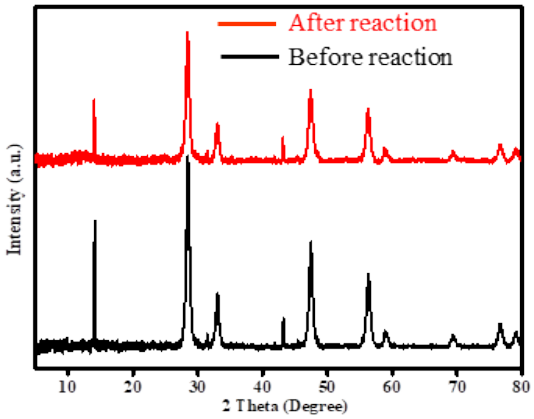

Fig. S12. XRD spectra of MC-2 before, and after reaction.

Table S4. Respective H_2O_2 production rate of all prepared samples using different sacrificial agent.

Photocatalysts	H_2O_2 evolution rate (μmol/h/g) using different sacrificial agent		
	MeOH	**EtOH**	**IPA**
C/N-CeO_2	1183.6	992.8	1342.5
MIS	389.1	312.4	545.7
MC-1	1603.7	1478.9	2115.2
MC-2	**2067.6**	**1884.3**	**2520.4**
MC-3	1715.3	1567.3	2383.0

Table S5. Comparison of photocatalytic H_2 evolution rate of different catalysts.

Photocatalyst	**Light source**	**Sacrificial agent**	**H_2 Production rate (μmol/h)**	**Ref.**

CeO_2/g-C_3N_4	300 W Xenon lamp	TEOA (triethanolamine)	203.6	[9]
TiO_2/MoS_2/Graphene	350 W Xe lamp	C_2H_5OH	165.3	[10]
α-MnO_2 @B/O-g-C_3N_4	125 W Hg lamp	CH_3OH	560.1	[11]
CeO_2@MoS_2/g-C_3N_4	3 W UV-LEDs	$Na_2SO_3$and Na_2S	65.4	[12]
1T/2H-MoS_2@CeO_2	Visible spectrum	0.5M Na_2S/Na_2SO_3	73.1	[13]
C/N- CeO_2/MIS	125 W Hg lamp	CH_3OH	419.2	This work

Table S6. Comparison of photocatalytic O_2 evolution rate of different catalysts.

Photocatalyst	**Light source**	**Sacrificial agent**	**O_2 Production rate (μmol/h)**	**Ref.**
CuO/CeO_2	300 W Xe lamp	NaOHand $Na_2S_2O_8$	19.6	[14]
α-MnO_2 @B/O-g-C_3N_4	150 W Hg lamp	$AgNO_3$	295.1	[11]
$ZnCr_2O_4$@ZnO/g-C_3N_4	Visible light (λ ≥ 400 nm)	$AgNO_3$	227.5	[15]
CeO_2/UNH (Ce)	125 W Hg lamp	$FeCl_3$	370.2	[1]
C/N- CeO_2/MIS	125 W Hg lamp	$AgNO_3$	210.1	This work

Table S7. Comparison of photocatalytic H_2O_2 production rate of different catalysts.

Photocatalyst	**Light source**	**Sacrificial agent**	**H_2O_2 Production rate (μmol/g/h)**	**Ref.**
CeO_2 / $SnIn_4S_8$	Visible light	No sacrificial agent	33.6	[16]

C/N-ZnO@NixPy	250 W Hg lamp	Ethanol	2495.1 ± 62.3	[5]
$MgIn_2S_4$@BCN	250 W Hg lamp	Ethanol	2175	[7]
TiO_2@MXene/B-g-C_3N_4	250 W Hg lamp	Ethanol	1480.1	[17]
Fe_2O_3/BCN	250 W Hg lamp	IPA	729	[18]
Mn_3O_4/ Co_9S_8	Xe lamp > 420 nm	Ethanol	1020	[19]
C/N- CeO_2/MIS	250 W Hg lamp	IPA	2520.4	This work

Table S8. Details of Chemicals and Instruments used.

Sl No.	**Chemicals/ Instruments**	**Manufacturer**	**City and Country**
1	Cerium chloride, 2-Amino-1,4-benzeen dicarboxylic acid, Magnesium nitrate, Indium nitrate, Thioacetamide	Sigma-Aldrich	Burlington, United states
2	Methanol, and N, N-Dimethyl formamide	Merck	Darmstadt, Germany
3	X-Ray Diffraction (XRD)	Rigaku-Ultima IV	Tokyo, Japan
4	UV–Visible (UV–Vis) diffuse reflectance spectra (DRS)	JASCO V-750	Halifax, Canada
5	Fourier Transform Infrared spectrometer (FTIR)	JASCO FTIR-4600	Halifax, Canada
6	Photoluminescence Spectrofluorometer (PL)	JASCO FP-8300 spectrofluorometer	Halifax, Canada
7	Raman spectrometer	RENISHAW InVia Raman spectrometer	Wotton-under-Edge, England
8	Electrochemical analyser	IVIUMnSTAT	Eindhoven, Netherland

9	Transmission electron microscopy (TEM)	TEM,JEOL-2100	Tokyo, Japan
10	Field Emission Scanning Electron Microscope (FESEM)	Zeiss, Gemini-300	Jena, Germany
11	Electron paramagnetic resonance spectrometer (EPR)	Bruker, ELEXSYS	Billerica, United states
12	Zeta potential	Zetasizer Nano ZS	Malvern, United Kingdom

References:

1 S. Mansingh, S. Subudhi, S. Sultana, G. Swain and K. Parida, *ACS Appl. Nano Mater.*, 2021, **4**, 9635–9652.

2 T. Tang, X. Jin, X. Tao, L. Huang and S. Shang, *J. Alloys Compd.*, 2022, **895**, 162452.

3 S. P. Tripathy, S. Subudhi, A. Ray, P. Behera, A. Bhaumik and K. Parida, *Langmuir*, 2022, **38**, 1766–1780.

4 X. Cheng, X. Yu and Z. Xing, *Appl. Surf. Sci.*, 2012, **258**, 3244–3248.

5 A. Ray, S. Subudhi, S. P. Tripathy, L. Acharya and K. Parida, *Adv. Mater. Interfaces*, , DOI:10.1002/admi.202201440.

6 G. Swain, S. Sultana and K. Parida, *ACS Sustain. Chem. Eng.*, , DOI:10.1021/acssuschemeng.9b07821.

7 L. Acharya, G. Swain, B. P. Mishra, R. Acharya and K. Parida, *ACS Appl. Energy Mater.*, 2022, **5**, 2838–2852.

8 S. P. Tripathy, S. Subudhi, A. Ray, P. Behera, G. Swain, M. Chakraborty and K. Parida, *Langmuir*, 2023, **39**, 7294–7306.

9 S. Zhang, J. Guo, W. Zhang, H. Gao, J. Huang, G. Chen and X. Xu, *ACS Sustain. Chem. Eng.*, 2021, **9**, 11479–11492.

10 H. H. Do, D. L. T. Nguyen, X. C. Nguyen, T. H. Le, T. P. Nguyen, Q. T. Trinh, S. H. Ahn, D. V. N. Vo, S. Y. Kim and Q. Van Le, *Arab. J. Chem.*, 2020, **13**, 3653–3671.

11 B. P. Mishra, L. Acharya, S. Subudhi and K. Parida, *Int. J. Hydrogen Energy*, 2022, **47**, 32107–32120.

12 C. Zhu, Y. Wang, Z. Jiang, F. Xu, Q. Xian, C. Sun, Q. Tong, W. Zou, X. Duan and S. Wang, *Appl. Catal. B Environ.*, 2019, **259**, 118072.

13 C. Zhu, Q. Xian, Q. He, C. Chen, W. Zou, C. Sun, S. Wang and X. Duan, *ACS Appl. Mater. Interfaces*, 2021, **13**, 35818–35827.

14 V. I. Markoulaki, I. T. Papadas, I. Kornarakis and G. S. Armatas, *Nanomaterials*, 2015, **5**, 1971–1984.

15 S. Patnaik, D. P. Sahoo, L. Mohapatra, S. Martha and K. Parida, *Energy Technol.*, 2017, **5**, 1687–1701.

16 Y. Xiao, Y. Tao, Y. Jiang, J. Wang, W. Zhang, Y. Liu, J. Zhang, X. Wu and Z. Liu, *Sep. Purif. Technol.*, 2023, **304**, 122385.

17 B. P. Mishra, L. Biswal, S. Das, L. Acharya and K. Parida, *Langmuir*, , DOI:10.1021/acs.langmuir.2c02315.

18 Z. Lu, X. Zhao, Z. Zhu, Y. Yan, W. Shi, H. Dong, Z. Ma, N. Gao, Y. Wang and H. Huang, *Chem. - A Eur. J.*, 2015, **21**, 18528–18533.

19 H. Zhang and X. Bai, *Appl. Catal. B Environ.*, 2021, **298**, 120516.